PNAS RESEARCH ARTICLE | NEUROSCIENCE

Visual guidance fine-tunes probing movements of an insect appendage

Sören Kannegieser[a], Nadine Kraft[a], Alexa Haan[a], and Anna Stöckl[a,b,c,1]

Edited by John Hildebrand, The University of Arizona, Tucson, AZ; received April 28, 2023; accepted December 13, 2023

Visually guided reaching, a regular feature of human life, comprises an intricate neural control task. It includes identifying the target's position in 3D space, passing the representation to the motor system that controls the respective appendages, and adjusting ongoing movements using visual and proprioceptive feedback. Given the complexity of the neural control task, invertebrates, with their numerically constrained central nervous systems, are often considered incapable of this level of visuomotor guidance. Here, we provide mechanistic insights into visual appendage guidance in insects by studying the probing movements of the hummingbird hawkmoth's proboscis as they search for a flower's nectary. We show that visually guided proboscis movements fine-tune the coarse control provided by body movements in flight. By impairing the animals' view of their proboscis, we demonstrate that continuous visual feedback is required and actively sought out to guide this appendage. In doing so, we establish an insect model for the study of neural strategies underlying eye-appendage control in a simple nervous system.

visually guided reaching | visuomotor control | insect | hawkmoth | proboscis

Significance

Visually guided reaching of a hand or other appendage comprises an intricate neural control task. Invertebrates, with their numerically constrained central nervous systems, are often considered incapable of this level of visuomotor control. Here, we provide mechanistic insights into visual appendage guidance in insects by studying the probing movements of the hummingbird hawkmoth's proboscis as they search for a flower's nectary. We show that visually guided proboscis movements fine-tune the coarse control provided by flight. By impairing the animals' view of their proboscis, we demonstrate that continuous visual feedback is required and actively sought out. These results establish an insect model for the study of neural strategies underlying eye-appendage control in a simple nervous system.

Visually guided reaching—to our coffee cup or a button on our phone display—is a key feature of human life (1) and increasingly frequent in robotic applications (2). It comprises an intricate neural control task, including visually identifying the target's position in 3D space, passing the representation to the motor system, and enacting control commands to the respective appendages (3–6). Ongoing movements are adjusted via visual and proprioceptive feedback to minimize errors (7–9). Given the complexity of the neural processing involved, visually guided appendage movements are thought to require substantial neural resources and are correspondingly found particularly in mammals and birds—including the guidance of forelimbs (10) or beaks (11, 12). Invertebrates, with their numerically smaller central nervous systems, are often considered incapable of this level of visuomotor control, instead relying strongly on stereotyped motor patterns under peripheral nervous control.

Yet, vision plays an important role in invertebrate locomotion and can elicit reaching movements, particularly to strike at prey or stride across gaps. Striking movements are often executed in a ballistic fashion once triggered: Praying mantids, octopuses, and cuttlefish use vision to gauge the suitability and direction of a target before they strike at it (13–15). Similar to locusts, horse-headed grasshoppers, and fruit flies, which adjust the length of their foreleg strides to the visually estimated distance of a gap (16–18), praying mantids can adjust the reach of their ballistic strike at prey with distance (19). Yet, there is only one known instance of continuous visually guided appendage movements in insects: Crickets and cockroaches point single antenna to a visual object and track its movement (20, 21), likely to optimally position the antenna for mechanosensory inspection (22). Exceptional in terms of visual appendage guidance among invertebrates is the common octopus, which relies on vision to move its arms through a maze (23). While likely under continuous proprioceptive control (24, 25), none of these invertebrate behaviors has been shown to require visual feedback to continuously monitor the position of the appendage during its movement, a hallmark in primate visual appendage guidance (7–9).

A continuous appendage guidance behavior that lends itself ideally to investigate visual guidance and the role of visual feedback, is the proboscis inspection of flowers by hovering hawkmoths (26–29). These insects hover in front of flowers while maneuvering their long proboscis into the nectary (30), thus requiring both 3D flight control and proboscis guidance, as well as coordination between both motor tasks during flower inspection. There is strong evidence that both body and proboscis guidance require vision: It has been shown that nocturnal hawkmoths use visual patterns to align their body when inspecting flowers (26). Moreover, the diurnal hummingbird hawkmoths (*Macroglossum stellatarum*) target visual features upon their first proboscis contact with flowers (28). Building on

Author affiliations: [a]Behavioral Physiology and Sociobiology (Zoology II), University of Würzburg, Biozentrum am Hubland, Würzburg 97074, Germany; [b]Department of Biology, University of Konstanz, Konstanz 78464, Germany; and [c]Zukunftskolleg, Universität Konstanz, Konstanz 78464, Germany

Author contributions: A.S. designed research; S.K., N.K., and A.H. performed research; S.K., N.K., A.H., and A.S. analyzed data; and S.K., N.K., A.H., and A.S. wrote the paper.

The authors declare no competing interest.

This article is a PNAS Direct Submission.

[1]To whom correspondence may be addressed. Email: anna.stoeckl@uni-konstanz.de.

This article contains supporting information online at https://www.pnas.org/lookup/suppl/doi:10.1073/pnas.2306937121/-/DCSupplemental.

Published January 29, 2024.

these insights, we mechanistically dissected the proboscis flower probing behavior of hummingbird hawkmoths to isolate the contribution of visual flight control and proboscis guidance in targeting visual cues. By impairing the animals' view of their proboscis during probing, we provide evidence that online visual feedback of the proboscis is required and actively sought out for the guidance of this appendage.

Results

Hawkmoths Targeted Visual Flower Patterns with Their Proboscis. To reveal whether hummingbird hawkmoths control their proboscis visually when probing flowers, we used high-speed video tracking of their head, thorax, and proboscis tip as they probed different types of artificial flower patterns in flight (Fig. 1 *A* and *B* and *SI Appendix*, Fig. S1 *A* and *B*). For all visual pattern shapes tested, the resulting proboscis contacts were placed on the patterns significantly more often than on the flower background (Fig. 1 *C–F*, for statistical results, see *SI Appendix*, Table S1), provided that the moths could resolve the pattern features (at least 0.25 mm width, corresponding to 0.7° of visual angle, *SI Appendix*, Fig. S2). On flowers without a pattern, proboscis contacts were homogeneously distributed over the flower's surface (Fig. 1*F*). Since no olfactory cue or sugar reward was presented during these tests, and all artificial flowers had the same mechanosensory surface properties, we concluded that proboscis placement during flower probing must have been visually controlled.

While the proboscis targeting of visual patterns suggests active visual proboscis control, alternative motor strategies could explain these observations: As the animals hover at the flowers during probing, their body movements could passively direct the proboscis onto the target locations, and their proboscis could be indirectly moved as a result of head movements. Indeed, the proboscis movement trajectories showed similar low temporal frequency components as the trajectories of head and thorax during flower probing (Fig. 1*G*). However, comparing the amplitude of thorax and head movements to proboscis movements (amplitude spectrum of the proboscis, head, and thorax for individual animals *SI Appendix*, Fig. S3, for all animals *SI Appendix*, Fig. S4 *A–D*) demonstrated that proboscis movements were not mirroring the movement of either thorax (Fig. 1*H*) or head (*SI Appendix*, Fig. S4*B*). They had smaller amplitudes at frequencies lower than 3.5 Hz and exceeded these at higher frequencies, suggesting that the proboscis tip moved under separate motor control from the head and thorax.

The Hawkmoths' Proboscis Moved Actively and in Coordination with Body Movements. To characterize proboscis movements independent of body movements which passively moved the proboscis, we transformed the proboscis, head, and thorax positions to a new coordinate system defined by the head–thorax axis (*SI Appendix*, Figs. S4*E* and S5*B*). The distinct amplitude and frequency spectrum of proboscis movements in the head–thorax reference frame (*SI Appendix*, Fig. S4*F*) suggest that these movements were active, enacted by proboscis muscles. The amplitude of proboscis movements parallel to the head–thorax axis was well in agreement with the range of extension of the proboscis along that axis (ca. 25 mm, depending on the size of the animal) and previous descriptions of proboscis movements in Lepidoptera (31, 32). The movements perpendicular to the head–thorax axis, while significantly smaller than parallel ones (*SI Appendix*, Fig. S4*G*), still had amplitudes of several millimeters, which might not be expected given the distribution of muscles in the hawkmoth proboscis (33). These movements might have been generated either actively, or by head movements, such as yaw, pitch, or roll rotations relative to the thorax, which then passively moved the proboscis.

To quantify head rotations, we tracked three additional landmarks on the heads of a subset of hawkmoths: the frontal tip of the head (*SI Appendix*, Fig. S5*A*), where the proboscis base connect, and the left and right base of the antenna. This generated direct means to quantify the anterior–posterior head axis (*SI Appendix*, Fig. S5*A*, green line), in addition to estimates of roll and yaw rotations of the head. Such head rotations were quantified in the

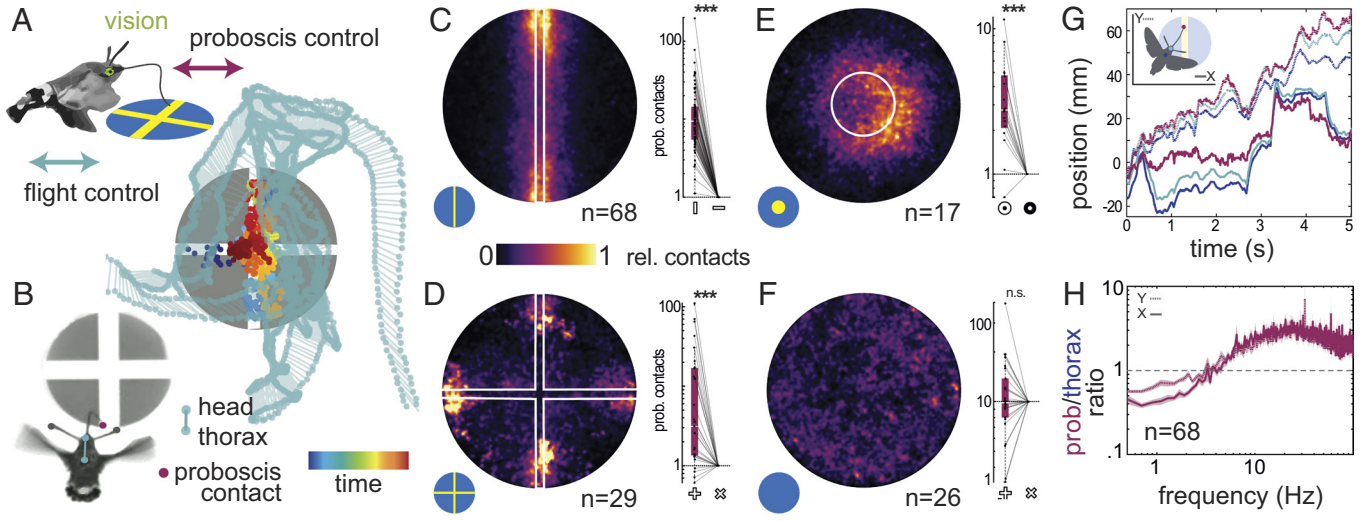

Fig. 1. Hawkmoths probe visual flower patterns with their proboscis. (*A*) Hawkmoths insert their long proboscis into the nectary of flowers while hovering in front of them. In principle, proboscis insertion requires guidance by flight maneuvers but might also involve active control of the proboscis. (*B*) To examine visuomotor control in this task, we analyzed both the moths' body position in the air and proboscis movements on the flower using high-speed video tracking of the head, thorax, and proboscis tip during flower probing. (*C–F*) Proboscis contacts on artificial flower patterns (symbols depict pattern types), normalized and averaged across individuals (n). The *Insets* for line and cross patterns and the pattern-less condition show the number of proboscis contacts ±2 mm off the pattern axes, compared to the same area rotated 90° or 45°, respectively (see symbols below the graph). For the circle pattern, the number of contacts on the pattern was compared to those on the background, normalized by the respective areas. Statistical comparisons were performed using Wilcoxon signed-rank tests (*SI Appendix*, Table S1). Their results are abbreviated as * ($P < 0.05$), ** ($P < 0.01$), *** ($P < 0.001$), and n.s. (not significant). (*G*) Example of the trajectory of the thorax (dark blue), head (light blue), and proboscis (purple), and (*H*) ratio of the amplitude spectrum of proboscis and thorax movements during flower probing (*SI Appendix*, Fig. S3).

head–thorax reference frame (*SI Appendix*, Fig. S5*B*, body axis coordinates). Changes in the lateral distance between the antenna base tracking points were used as a measure for head roll, and changes in the distance between the proboscis base and head tracking point for head pitch. Both changes in the anterior–posterior distance between antenna bases, as well as the angular displacement of the proboscis base from the head–thorax axis, were used as measures for head yaw (*SI Appendix*, Fig. S5 *B*, *Insets*).

Both measures of head yaw rotations showed distinct temporal coherence with proboscis movements perpendicular to the head–thorax axis (*SI Appendix*, Fig. S5*E*, green; *SI Appendix*, Fig. S5*F*, red). The same was true for lateral movements of the head base and the proboscis relative to the head–thorax axis (*SI Appendix*, Fig. S5*E*, solid black), demonstrating that a portion of lateral proboscis movements occurred in conjunction with head yaw rotations. There was no coherence between head roll and proboscis movements perpendicular to the head–thorax axis (*SI Appendix*, Fig. S5*F*, orange line), or head pitching movements and proboscis movements parallel to the head–thorax axis (*SI Appendix*, Fig. S5*E*, dashed black line).

Temporal coherence between proboscis movements perpendicular to the head–thorax axis and head yaw rotations does not mean that head yaw generated these proboscis movements. They might also have been generated by body movements lateral to the probing proboscis, which coincided with or caused head yaw rotations. To resolve these two possibilities, we analyzed the temporal coherence between the angular rotation of the thorax (in the flower reference frame) and of the proboscis base relative to the body axis (*SI Appendix*, Fig. S5*G*, green) and for lateral proboscis movements relative to the body axis (*SI Appendix*, Fig. S5*H*, brown), respectively. Their similarity in temporal coherence suggests that lateral proboscis movements, as well as head yaw rotations, indeed coincided with body rotations. This effect was specific to rotations, as absolute thorax displacements had no coherence with lateral proboscis movements (*SI Appendix*, Fig. S5*I*, blue line). Neither did absolute proboscis displacements (*SI Appendix*, Fig. S5*I*, purple line)—which would have been expected if lateral proboscis movements relative to the head–thorax axis were caused by active proboscis movements off the body's midline, rather than displacements of the body lateral to the proboscis.

Thus, we concluded that hawkmoths actively moved their proboscis most strongly parallel to the head–thorax body axis, while body rotations around the probing proboscis generated a portion of the lateral proboscis positions relative to the body axis. These coincided with head rotations, likely due to the fixed relationship between the head and proboscis, which forced the head to rotate to stay in line with the proboscis while the body rotated around the probing proboscis. Consequently, to understand visual proboscis targeting, both proboscis and flight movements had to be taken into account.

Hawkmoths Used Flight Control to Coarsely Position Their Proboscis on Flower Patterns. To assess what role flight control played in passively positioning the proboscis onto flower patterns, we analyzed the animals' body orientation with respect to the visual patterns during flower approach (250 ms immediately before proboscis contact), probing phase and upon departure (250 ms after the last proboscis contact, Fig. 2*A*). The animals' head-to-thorax body axis was significantly aligned with the pattern axis during the approach, but not the departure (Fig. 2 *B* and *D*, for statistical results, see *SI Appendix*, Table S2). Approach alignment did not require the patterns to extend to the rim of the flower, as long as they had a clear directionality (*SI Appendix*, Fig. S4, middle

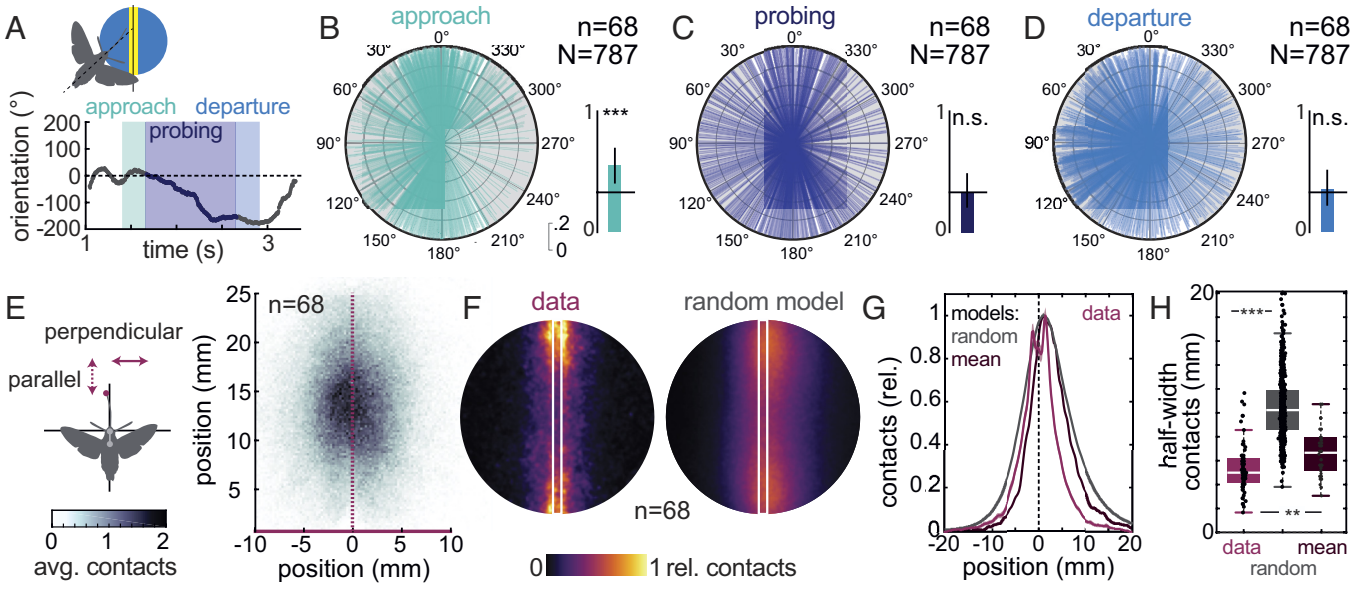

Fig. 2. Hawkmoths used flight control to coarsely position their proboscis on flower patterns. (*A*) The hawkmoths' head-to-thorax body orientation relative to the pattern orientation in three different stages of flower interaction: the approach 250 ms immediately before proboscis contact (turquoise), the departure 250 ms immediately after the last proboscis contact (blue), and the probing time in between (dark blue). (*B–D*) The animals' orientation during the approach, probing, and departure. Each line represents a probing trial (N) of one animal (n). The *Inset* bar graphs depict the results of a statistical test (GLMM with binomial distribution, see *Materials and Methods*, *SI Appendix*, Table S2) to assess whether the hawkmoths' body orientation fell into the pattern sectors (white background) significantly more frequently than chance. Depicted are the mean and CI of the probability of body orientations within pattern sectors, as well as the prediction for random orientations (black line). (*E*) To generate a prediction of the hawkmoths' proboscis positions based on passive movement by the body in flight, the proboscis positions relative to the body were extracted for each video frame. (*F*) Relative proboscis positions were then randomly assigned to a body position for each frame of a probing trial video (as in Fig. 1*C*, data). Ten iterations of this random assignment were generated for each trial of each animal (model). (*G*) The relative number of contacts summed along the pattern axis for the data and random model, as well as a model based on the mean proboscis position of each animal. Shown are the mean and SEM. (*H*) Half-width of the contact distribution depicted in (*G*) for all flower probing trials (*N*) of all animals (*n*). A Mann–Whitney rank-sum test was used for statistical comparison of the data and random model (N = 787, z-score = −11.86, $P < 0.001$) and a signed-rank test for the paired data and mean model (z-score = −2.62, $P = 0.009$). Statistical results are abbreviated as * ($P < 0.05$), ** ($P < 0.01$), *** ($P < 0.001$), and n.s. (not significant).

row). Thus, the hawkmoths used the directional information in the patterns to align their body upon the approach, which might aid the subsequent pattern probing.

Intriguingly, the body axis of the animals was not consistently aligned with the patterns in the probing phase (Fig. 2*C*), demonstrating that the animals did not simply target their proboscis onto the pattern by moving their body along the pattern axes. To test whether the moths used more intricate flight maneuvers to passively target their proboscis on the patterns, we generated a prediction of proboscis placements that was purely based on flight control. We extracted the proboscis position relative to the body for each video frame of each trial (Fig. 2*E*) and then randomly assigned these relative proboscis positions to the animals' body positions on a frame-by-frame basis, separately for each animal (Fig. 2*F*, random model). This prediction, which assumed that proboscis movements were random, captured the general structure of the recorded proboscis placements very well (Fig. 2*F*). However, unlike the data, the modeled proboscis contact distribution was not centered with the pattern and did not contain the distinct peaks that aligned with the pattern edges (Fig. 2*G*, gray). Moreover, the modeled contact distribution was significantly wider (Fig. 2*H*). A further model, based on assigning the mean proboscis position of each animal to its body position throughout the trial, similarly resulted in an off-centered distribution which did not recapitulate the distinct pattern edge contacts in the data (Fig. 2*G*, dark purple) and also resulted in a significantly wider contact distribution than the data (Fig. 2*H*). Together, these results demonstrate that purely passive, flight-based proboscis placement could not have generated the precise and highly structured proboscis contacts we observed.

Hawkmoths Used Visually Guided Proboscis Movements to Fine-Tune Probing Position. We hypothesized that the proboscis might be coarsely targeted to visual patterns by flight maneuvers, and that active visual proboscis guidance fine-tuned the probing positions. This hypothesis was also supported by the movement kinematics of the proboscis, which were distinct from those of the animals' body, with greater relative amplitudes at higher temporal frequencies (Fig. 1*H*). To assess whether these kinematics were random search movements, or whether they were directly visually guided, we isolated the hawkmoths' proboscis targeting from their flight control. To do so, we enclosed the artificial flowers within a confining corridor, in which the moths could not turn in flight. Thus, their head–thorax body axis remained parallel to the corridor axis. By orienting the pattern axis parallel (Fig. 3*A*) or perpendicular (Fig. 3*B*) to the corridor, the animal thus had to perform proboscis movements with more parallel or perpendicular components, respectively, relative to their body axis, for optimal pattern probing. The contact distributions revealed that the animals' probing precision was much higher with parallel rather than perpendicular patterns (Fig. 3 *A* and *B*, *Left*). Yet, in both cases, the contact distributions were centered on the pattern (Fig. 3 *C* and *F*), and the contrast distribution in the perpendicular condition showed peaks at the pattern edges, suggesting that the animals did target the pattern with the same strategy as in free flight (Fig. 2*G*).

The proboscis contact distributions in both the parallel and perpendicular conditions were significantly narrower than the ones predicted for random proboscis movements (Fig. 3 *D* and *G*). Moreover, in the perpendicular condition, which provided the more challenging control task, since body movements in the pattern direction were constrained, the model prediction without proboscis guidance was strongly off-center from the pattern (Fig. 3*G*). This demonstrates that the animals adjusted their probing positions using visually targeted proboscis control. It was further confirmed by calculating the ratio of parallel to perpendicular proboscis movements relative to the body axis (Fig. 3*H*). To optimally probe the patterns, more parallel than perpendicular proboscis movements

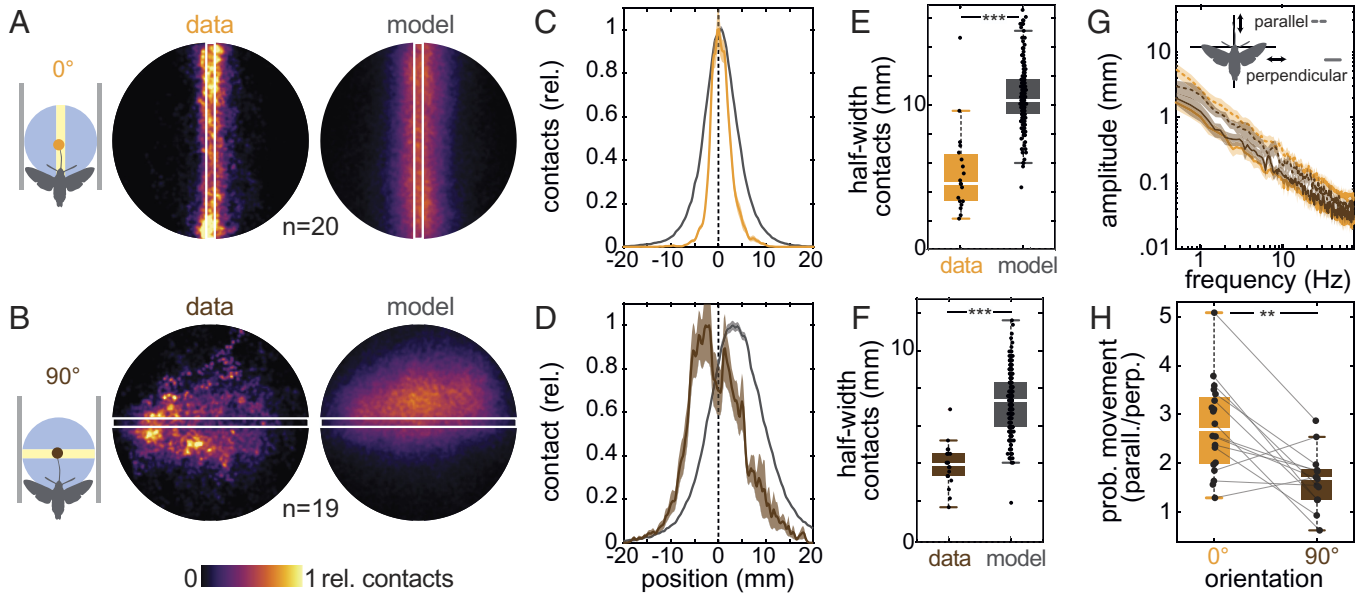

Fig. 3. Hawkmoths used visually guided proboscis movements to fine-tune their probing. (*A* and *B*) To isolate the hawkmoths' proboscis movements from their flight maneuvers, a corridor surrounding the artificial flowers confined the moths' head–thorax axis parallel to the corridor axis. Orienting the pattern axis parallel (*A*, 0°) or perpendicular (*B*, 90°) to the corridor required the animals to perform proboscis movements with more parallel or perpendicular components relative to their body axis for optimal pattern probing. Normalized contact distributions (data, *Left* panels) and a prediction of random proboscis placement (model, *Right* panels, see *Materials and Methods* and Fig. 2 *E* and *F*) are shown for both conditions. (*C* and *D*) The relative number of contacts summed along the pattern axis for the data (brown hues) and model (gray). Shown are the mean and SEM. (*E* and *F*) Half-width of the contact distribution depicted in (*C* and *D*) for all flower probing trials of all animals (*n*). A Mann–Whitney rank-sum test was used for statistical comparison (n_{data} = 20, n_{model} = 200, z-score = −6.76 and n_{data} = 19, n_{model} = 190, z-score = −6.07). (*G*) The amplitude of proboscis movements parallel (dashed) and perpendicular (solid) to the body orientation in the 0° (orange) and 90° (brown) conditions. Their ratio is depicted in (*H*). Statistical comparison was performed using a Wilcoxon signed-rank test (n_0 = 20, n_{90} = 19, z-score = −11.86, *P* = 0.003). All statistical results are abbreviated as * (*P* < 0.05), ** (*P* < 0.01), *** (*P* < 0.001), and n.s. (not significant).

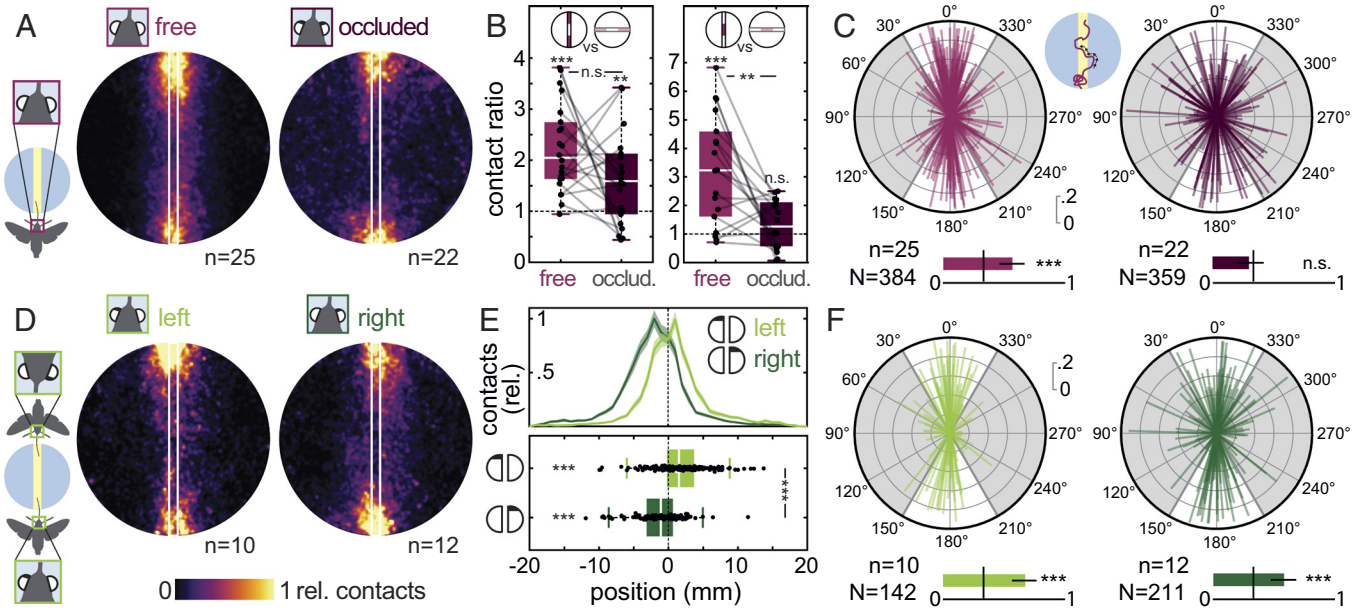

Fig. 4. Visual feedback is required for proboscis targeting. (*A*) To obstruct the hawkmoths' view of their proboscis during probing, their fronto-visual field was occluded in both eyes by applying black paint. Normalized contact densities of the control condition with free eyes (*Left*), and with occluded visual field (*Right*). (*B*) Ratio of proboscis contacts on the pattern (dark shaded *Inset*) versus the respective 90° rotated area (light shaded *Inset*) for the free and occluded treatment. Contacts scored in the outer thirds (*Left*) and in the central third (*Right*) of the pattern. Statistical comparisons were performed using Wilcoxon signed-rank tests (*SI Appendix*, Table S3). (*C*) The mean vector of the hawkmoths' proboscis tracks for all animals (*n*) and flower approaches (*N*) with free and occluded frontal visual fields. Pattern sectors are in white, background sectors in gray. The *Inset* bar graphs depict the results of a statistical test (GLMM with binomial distribution, see *Materials and Methods*, *SI Appendix*, Table S4) to assess whether the mean probing direction aligned with the pattern sectors. Depicted are the mean and CI of this probability, as well as the prediction for random orientations (black line). (*D*) Proboscis probing positions with either the right or left frontal visual field occluded. (*E*) Distribution of proboscis contacts (mean and SEM) summed along the pattern axis for animals with left (light green) and right (dark green) occlusion. The *Lower* panel shows the position of the median of the contact distribution for all trials. Statistical analysis comparing the median probing positions was performed by a Mann–Whitney rank-sum test. A Wilcoxon signed-rank test was used to compare the median positions to the pattern axis midline (*SI Appendix*, Table S3). (*F*) Mean vector of the proboscis probing tracks for all trials with left and right occlusion. The statistical results are depicted as in (*C*) and abbreviated as * < 0.05, ** < 0.01, *** < 0.001, and n.s. not significant.

would be required in the parallel condition and vice versa in the perpendicular condition. This was indeed the case (Fig. 3*H*), confirming that the animals tuned their proboscis movements to the visual cues to optimally target the patterns.

Continuous Visual Feedback Is Required for Proboscis Targeting. Having established that the animals use flight control for coarse visual targeting, but rely on visual proboscis guidance to fine-tune their probing position, we next wondered whether these processes require the moths to see their proboscis on the flower during probing. To test the need for visual feedback, we occluded the hawkmoths' view of their the proboscis, using black paint on the fronto-ventral portion of their eyes (Fig. 4 *A* and *B* and *SI Appendix*, Fig. S8 *D* and *E*). We first tested animals with free eyes, then occluded either their left or right visual field (Fig. 4*B*), to finally test them with both eyes occluded (Fig. 4*A*). Similarly to the free condition, animals with the frontal visual field in both eyes occluded still approached and probed the artificial flowers (Fig. 4*A*) for a similar length of time as with free eyes (*SI Appendix*, Fig. S6*C*). Importantly, they also aligned their body axis with the pattern upon their approach flight (*SI Appendix*, Fig. S5*B*) and established the initial contact with the flower at the intersection of the patterns and the edge of the flower. These observations confirm that the animals were able to see the pattern on the flower, despite the occlusion of their fronto-ventral visual field. While animals with occluded eyes still contacted the outer part of the patterns significantly more than the background (Fig. 4 *B*, *Left*), this was not the case for the central part of the pattern (Fig. 4 *B*, *Right*). Consequently, there was no significant difference in proboscis contacts for the outer pattern portion compared to animals with free eyes (Fig. 4 *B*, *Left*), but a significant difference in the central pattern portion (Fig. 4 *B*, *Right*). This suggests that the animals with an occluded view of their proboscis were not able to probe along the patterns (toward the flower's center) after establishing the initial contact at the flower edge.

We further confirmed this hypothesis by analyzing the average direction of the animals' proboscis probing tracks (Fig. 4*C*). If the animals probed along the patterns, the average direction of the resulting probing vector should be aligned with the patterns' orientation. This was indeed the case for animals with free eyes, but not for animals with occluded eyes, confirming that visually guided proboscis probing requires a view of the proboscis on the flower. Indeed, we noticed that the animals actively sought out this view, by moving their proboscis into the free visual field when only one eye was occluded (Fig. 4*D*). Animals with their left eye occluded contacted the visual patterns to the right of the pattern center and vice versa for animals with their right eye occluded (Fig. 4 *E*, *Upper*). The median of the contact distributions in each treatment was significantly displaced from the pattern center and differed significantly between left and right treatments (Fig. 4 *E*, *Lower*). The median proboscis position relative to the animals' body axis was shifted correspondingly (*SI Appendix*, Fig. S6*A*) and significantly correlated with the shift in position relative to the pattern (*SI Appendix*, Fig. S6*B*). In both cases, the mean vector of the animals' proboscis tracks was aligned with the pattern axis (Fig. 4*F*), demonstrating that hawkmoths could guide their proboscis along the patterns with only one free eye.

Discussion

Here, we demonstrated how the hummingbird hawkmoth *M. stellatarum* targets visual cues with their proboscis, achieving coarse target guidance with flight movements and fine-tuning of the probing

position through visually guided proboscis movements. We further showed that the moths require and actively seek out continuous feedback on the position of their proboscis to guide their probing. Providing mechanistic insights into continuous visual appendage guidance in insects, this finding poses a number of intriguing questions for future research and for comparisons to the well-studied control strategies in vertebrate appendage–eye coordination.

Motor Control of Proboscis Movements. While hawkmoths can precisely control their body in the air and even track moving objects in flight (34, 35), the movement range of the hawkmoth proboscis is much more limited. As in many other Lepidoptera which feature a bent proboscis, movements of the proboscis consist mainly of upward and downward motion at the proboscis base and forward–backward motion of the distal proboscis beyond the bend (31, 32). Corresponding to the distribution of muscles in the hawkmoth proboscis (33), lateral movements are possible to a much smaller degree. Our data confirm that movements parallel to the body axis have a twofold higher amplitude than lateral movements (*SI Appendix*, Fig. S3*B*).

How then do the animals achieve to probe flower patterns with high precision? This likely resulted from the interplay of body and proboscis movements—similar to the way our fingers can be moved on intricate trajectories, despite the relatively limited range of lateral motion in all fingers except the thumb—thanks to the interaction with hand and wrist movements (36). As our analysis of the role of head and body movements shows, lateral deviations of the proboscis from the animals' midline often occurred in conjunction with a rotation of the animal's body around its probing proboscis (*SI Appendix*, Fig. S5). Thus, hummingbird hawkmoths did not primarily move their head to target their proboscis to lateral positions outside of the movement range of proboscis muscles, but they rotated their bodies around the proboscis as they probed on the flower, showing an intricate interplay of proboscis targeting and flight maneuvers.

This raises the question, how flight and proboscis motor control is coordinated? For the primate hand, neural control is integrated across multiple joints at the same time, suggesting a concerted motor program for hand and finger movements (36). When hawkmoths track a moving flower while their proboscis is in contact with its nectary, mechanosensory feedback from the proboscis has different temporal kinematics to visual feedback (37). However, this paradigm is not directly comparable to our study since the proboscis is not actively moved, but contributes sensory feedback to flight control by passive deflections through flower movements. Nevertheless, we found a similar trend in our study: The temporal movement spectrum of the proboscis had distinctly higher amplitudes than that of the body for all frequencies above 4 Hz (Fig. 1*H*). Its broad and smooth frequency spectrum suggests that the proboscis was not under the control of a simple pattern generator, which would have resulted in one or more distinct frequency peaks. Given that the proboscis is also guided by mechanosensory cues (27, 29), it is conceivable that the movement pattern of the proboscis changes with different surface textures and 3D structures of the flower. Moreover, the movement patterns of the body and proboscis and their relative contributions to visual targeting might differ with the type of visual patterns, as well as the orientation of the flower—to optimally use the degrees of freedom and movement ranges of flight and proboscis control. Future research to reveal the—as yet unknown—origin of visual guidance commands to the proboscis will be key to understanding whether and how the motor commands for proboscis and body movements are coordinated during visually guided probing. Comparing their movement strategies to those of praying mantids, some of which use targeted body movements to aid their foreleg strikes (38–40), could be a powerful approach to reveal whether general mapping strategies for such visual targeting challenges exist across insects, or whether these differ depending on the appendage and behavioral task at hand.

Visual Control Strategies of Proboscis Probing. One aspect of the visual control strategy for proboscis probing that clearly emerged from our experiments was that the moths require a view of their proboscis with at least one eye. With both frontal visual fields occluded, the hawkmoths were not able to probe along the pattern—even though they still perceived the patterns when approaching and positioned their initial proboscis contacts onto them (Fig. 4). This suggests that hawkmoths might use a simple control strategy to guide their proboscis, in which they center the visual target in their frontal visual field and retain the view of both the proboscis and the target there. Since the proboscis is fronto-centrally located at the head, centering a visual target with respect to the head also automatically centers it to the proboscis' reference frame. A similar control strategy has been proposed for birds when pecking a target using visual control (11, 12). In general, controlling an appendage that is centrally attached to the head has the great advantage that a head-centered coordinate system applies, while reaching with a hand or arm might require a transformation from a head-centered to a hand-centered reference frame (41). Thus, the visual guidance of a beak or a proboscis might be conducted with less computational power than controlling a manipulator that moves independently of the head. The limited range of lateral proboscis movements could further reduce the complexity of the control task.

Our experiments also show that visual proboscis guidance does not require both eyes, which is similar to the antenna pointing behavior in crickets and cockroaches, which is also under single-eye control (20, 21). This might suggest that proboscis probing is indeed not head—but eye centered, relative to a (temporarily) dominant eye. Identifying the reference frame (head or eye) for proboscis guidance will lead to valuable insights into the underlying neural control. What can certainly be concluded from our results is that proboscis guidance does not require stereopsis. This is particularly different from striking tasks in other invertebrates, such as in praying mantids and cuttlefish, which use stereovision to assess the targets' distance (14, 15). Yet, when crossing gaps using visual guidance, horse-headed grasshoppers use parallax information generated by sideways peering movements rather than stereovision for distance estimation (17). We did not observe any sideways movements suited to parallax cue generation in hawkmoths approaching the visual targets—which might not have been necessary in this task since the proboscis provides a physical distance measure to the flower. Proprioceptors could provide information on the state of the proboscis (bent or fully extended), from which steering commands to keep the required distance to the flower to continue probing (*SI Appendix*, Fig. S5 *J* and *K*) could be extracted.

Proprioception could also provide important information about the position of the proboscis relative to the body, as is assumed to be for the antenna, moving legs, and striking forelimbs (20, 21, 24, 25, 40). Yet, our results clearly showed that visual feedback of the proboscis position is required for targeted probing, indicating that proprioceptive feedback is not sufficient for this task. It remains an open question how the animals perceive their proboscis. With less than 100 μm width in the hummingbird hawkmoths, it should be too narrow to resolve when fully or even half extended (at 20 to 10 mm distance from the eyes), given a maximum resolution of

ca. 1° in their frontal visual field (42). Hawkmoths might instead register the movement of the proboscis, which reaches amplitudes of more than 1 mm parallel to the body axis. Even the lateral movements of just 0.4 mm amplitude should still generate a detectable motion signal at full proboscis extension, which is within the spatial and temporal resolution limit of the hummingbird hawkmoth's motion vision system (43). The high contrast sensitivity of the hawkmoth's motion neurons further increases the likelihood that they can detect the moving proboscis tip.

The Role of Visual Feedback in Proboscis Guidance. In most examples of visual appendage control investigated to date, visual feedback is not necessary while the task is ongoing: In visually elicited targeting behavior, i.e., praying mantids or cuttlefish striking at a visual target (13–15), or pigeons pecking at a visual cue (11, 12), the motor action, once elicited, requires no further visual information. In all these examples, animals initially fixate the target and typically center it to their body, before initiating the movement of their appendages (or head in the case of birds). Unlike proboscis probing, these behaviors are not performed over longer periods of time, but either end successfully on catching the target, or if unsuccessful, require a new cycle of fixating and strike initiation. Hawkmoth proboscis probing, on the other hand, is a continuous visual search task, which requires a high degree of flexibility to adjust to different flower types and flower positions, so that a predefined movement sequence without feedback adjustment would likely not lead to a high frequency of successful outcomes.

Visual feedback during the ongoing motor action has been shown to improve precision of reaching and grasping in primate eye-hand coordination (44, 45), even though these species are capable of reaching without a current view of a briefly fixated target (46). While primates are capable of guiding their limbs to a memorized target position anywhere relative to the gaze direction, the opposite could be the case in hawkmoths: They might require their proboscis in view during probing because they cannot store an internal representation of the target and/or their proboscis and update it during the probing phase. Indeed, a similar strategy might be used by horse-headed grasshoppers crossing gaps, as they initiate the first step across the gap with the leg visible to their free eye upon single-eye occlusion (17). Keeping their moving appendage and the visual target at a fixed position in the visual field might be a straightforward control strategy for the seemingly complex task of visual appendage guidance used by insects. While this strategy would still require ongoing motor adjustments of the proboscis and the body in flight, as well as mutual coordination of proboscis and body movements, all movements would be performed within the same reference frame, and within the field of view of the same visual neurons. Based on our experiments, we cannot exclude that hawkmoths might be capable of memorizing the target position and shape. The occlusion of the frontal visual field in our experiment may have prevented the hawkmoths from performing the fixation that is required for goal directed appendage movements in primates and birds (11, 12). While they certainly saw the patterns and approached them during the initial flower contact, they may need to view cues with a specific frontal area of their visual field to be able to store a mental representation of the target. Future experiments occluding the target rather than the visual field will need to establish whether hawkmoths are capable of guiding their proboscis to a target when it is temporarily occluded, thereby helping to resolve the underlying proboscis control strategy. Revealing how such a complex task can be performed with the limited computational power of an insect will be extremely instructive in revealing fundamental strategies across animals of different brain size and manipulation complexity and can serve as a bioinspiration for the growing field of aerial manipulation in robotics (2, 47).

Materials and Methods

Animals. Male and female *M. stellatarum* (Sphingidae) were taken from a colony in Würzburg, Germany, which was raised on their native host plant *Gallium sp.* The adult animals were kept in flight cages (60 cm × 60 cm × 60 cm) on a 14:10 h light:dark cycle at 25 °C. They were fed with a 20% sucrose–water solution before experiments. Animals used in the experiments were between 3 d and 2 wk of age. At the start of each experiment, animals were separated into plastic vials, and handled individually throughout the experimental trials, to keep track of their identity.

Experimental Setup. Experiments were performed in a flight cage of 60 cm × 60 cm × 60 cm dimension at 25 °C (*SI Appendix*, Fig. S1*A*). The cage was lit from above with four 60 cm long daylight-like fluorescent tubes (Osram L 18 W/965 Biolux Tageslicht G13). All lights were connected to an electrical ballast (GloMat 2 × 40 W, Hagen), which increased the flicker frequency of the fluorescent tubes above 25 kHz, well outside of the resolvable range of the hawkmoths (30). A 25-cm high pedestal coated with white felt was placed in the center of the flight cage, on which the artificial flowers were mounted. The floor of the cage was lined with white paper tissue to present a uniform background for filming. A camera (acA 1300-200, Basler) was mounted directly above the ceiling of the flight cage, focusing on the artificial flower in the center of the cage (Fig. 1*B*). It was controlled using the Pylon Viewer Software (Basler) at 200 fps, with a field of view of 500 by 500 pixels (corresponding to ca. 12 × 12 cm in the focus plane, *SI Appendix*, Fig. S1*B*).

For the third experimental block (see below), a 10 cm long corridor was constructed out of black cardboard, into the center of which the artificial flower was placed (leaving no room between the edges of the flower and the corridor walls). The corridor walls extended 2.5 cm above the flower patterns. The corridor was sufficiently narrow that animals could fly to the flower, but were prevented from turning in the corridor without contacting the corridor walls with their wings, which the hawkmoths avoided. The corridor was not closed on the dorsal side, so the animals could exit it freely toward the ceiling of the cage. The height of the walls was chosen to ensure that the animals needed to fly within the corridor walls when probing the flower with their proboscis, thus fixing their body axis parallel to the corridor's main axis.

Stimuli and Visual Patterns. All artificial flowers were constructed from round paper cut-outs of 38 mm diameter, which falls into the preferred size range of flowers in this hawkmoth species (48). All stimuli were printed on unbleached paper ("Classic White," Steinbeis) using a laser color printer (C3325i, Canon). The yellow colors were set as C = 0%, M = 0%, Y = 100%, and K = 0% and the blue as C = 70%, M = 15%, Y = 0%, and K = 0%. The relative reflectance spectra of the resulting colors are shown in *SI Appendix*, Fig. S1*C*. They were laminated with a matt foil (S-PP525-22 matt, Peach, PRT GmbH) after printing and trimming and cut out to shape again.

All stimuli used in this study had a blue background, which was either presented as such (no pattern) or with different types of yellow patterns. Line patterns: A yellow line of 2 mm width was presented, either 38 mm long to extend over the entire diameter of the flower (Fig. 1*C*) or of 20, 10, 5, and 2 mm length (Fig. 1*E* and *SI Appendix*, Fig. S4). In addition, a 4-mm-wide and 38-mm-long yellow line was presented (Fig. 1*D*). Cross patterns: All yellow cross patterns extended over the entire diameter of the flower but varied in width from 0.125, 0.25, 0.5, 1, 2, 4, and 6 to 9 mm (Fig. 1*F* and *SI Appendix*, Fig. S2). In addition, a yellow circle of 12-mm diameter was used for comparison with the angular patterns (Fig. 1*G*).

Experimental Procedure. In this study, we performed four sets of experiments, in which different pattern types were shown to separate groups of hawkmoths (the number of all hawkmoths that performed in each experiment is provided in the respective figures). In the first experiment, line patterns of 2 mm width and varying length were presented. In the second experiment, cross patterns of varying width extending over the entire flower diameter were presented. In the third experiment, a line pattern of 2 mm was presented either oriented parallel or perpendicular to a corridor surrounding the artificial flower. In the fourth

experiment, a line pattern was presented without a surrounding corridor. The fronto-ventral area of the hawkmoths' eye was painted with black water–based lacquer to generate three subsequent testing steps in four resulting treatment groups: unpainted (all animals in the experiment), either the left or right eye was painted (the experimental group was split in either category), and both eyes were painted (all the remaining animals were tested in this condition). The animals were collected after both eyes were painted and their eyes were photographed from several orientations using a Flexacam C1 (Leica) camera mounted on a M80 stereomicroscope with 10× oculars and 1× objective (Leica).

In all experiments, the artificial flowers were presented without sugar water or odor cues. The flower patterns were rotated in their horizontal orientation between subsequent animals and days, to not be presented in the same orientation relative to the surrounding cage–except in the third experiment, where the pattern was specifically aligned to the corridor axis. The hawkmoths were released into the cage individually and given 10 min to approach the stimuli from flight onset. All approaches and probing phases within a session were recorded. Only one stimulus in one treatment group was tested per day. If an animal did not approach the flower in the allotted 10-min time slot, we repeated the same stimulus category the next day. If an animal did not perform on two consecutive days, it was excluded from the experiment. Animals were fed ad libitum with a 20% sugar solution after the experimental session and returned to their holding containers, which were placed in a dark box until the next experimental session.

Video Tracking. We used DeepLabCut (49) to automatically identify the proboscis, head, and thorax position of the hawkmoths (Fig. 1*B*). All videos were manually corrected for accuracy of the tracking points, particularly of the proboscis tip, which was only correctly identified automatically in a subset of frames, using the DLTdv7 software (50) in Matlab 2017b (The Mathworks). Only proboscis coordinates that were tracked when the proboscis was in contact with the artificial flower in the current frame or in the two frames before or after it were retained. Contact with the flower surface was noticeable in the small bend of the proboscis on its very tip. Using the same software, the flower position was marked by four points on the flowers' circumference parallel to the cardinal axes, and the pattern position was marked on all pattern edges in each video. Data were then further processed using custom-written Matlab scripts.

For a subset of animals, we also manually tracked the base of the left and right antenna, as well as the base of proboscis (where the proboscis connected to the head) for hawkmoths probing on line pattern flowers (*SI Appendix*, Fig. S5).

Data Analysis. For each animal (total number given as *n* in the figure legends), tracking data were generated for the head, thorax, and proboscis positions for each experimental session (presentation of a single pattern type in one experimental treatment). The same applied to the subset of animals, for which further head coordinates were tracked. Within a session, the hawkmoths generally approached the flowers multiple times, with varying lengths of probing times. Each of these individual approaches was registered as a trial (number given as *N* in the figure legends), which consisted of the approach flight (250 ms before the first proboscis contact), the probing phase (continuous proboscis contacts with the flower without interruption for more than 20 ms), and the departure phase (250 ms after last contact). Only animals with at least 500 proboscis contacts across all trials (corresponding to a total probing time of 10 s per condition) were included in the analysis.

Before further processing, all tracking points (of the hawkmoths and the flower) were rotated so that the long axis of the pattern was aligned with the y-axis of the cartesian coordinate system used throughout. Thus, the data were transferred from a cage-centric to a pattern-centric coordinate system. Where patterns had two possible axes for alignment (i.e., in cross-patterns), the minimum possible rotation of coordinates was used to align one of the pattern arms with the y-axis. Patterns without axial features (circles) and flowers without patterns were not rotated and remained in the camera frame of reference.

Proboscis contacts on the flower. To depict the distribution of proboscis contacts on the artificial flower patterns, the positions of the proboscis of each animal in all trials of a given pattern type were collected in a matrix, which represented the spatial layout of the flower. To compare animals with different numbers of proboscis contacts on the flower, contacts were summed for each animal, and then divided by the maximum number of contacts per animal. These normalized contact distributions were then averaged across animals, to generate the proboscis contact heatmaps (for example, Fig. 1 *C–H*).

To assess whether the animals used vision to guide their proboscis probing positions, we calculated two different types of metrics. For the first metric, we counted the number of contacts in an area ±2 mm around the central pattern axes for line and cross patterns. Unlike scoring contacts directly within the pattern area, this also included contacts that were placed close to, but not directly on the pattern, which was particularly frequent for fine patterns (Fig. 1 *C* and *F* and *SI Appendix*, Fig. S2 *B* and *C*). To assess whether the animals aligned their proboscis contacts with the pattern axes, we compared this contact count to the same area turned 90 degrees for line patterns, or 45 degrees for cross patterns (*Insets* in Fig. 1 *C–F*, and *H* and *SI Appendix*, Fig. S2). This analysis method was particularly sensitive for fine patterns, where the probing precision was not high enough to place the contacts directly onto the patterns, but the animals nevertheless aligned their proboscis contacts at the visual patterns, demonstrating visual guidance. The same analysis was also used to test for the directedness of pattern contacts in the no-pattern condition (Fig. 1*H*). A variation of this analysis was used to compare only the proboscis contacts in the outer thirds and inner third of the line pattern, with their respective 90° rotated areas (Fig. 4*B*). As a second metric, we counted the number of proboscis contacts of each animal on the pattern and compared it to the background, while scaling both counts for the respective areas (Fig. 1*G*).

For the line patterns, we also analyzed the placement of proboscis positions relative to the long pattern axis. To do so, we summed all proboscis contacts for each trial and each animal along the long pattern axis. We normalized this distribution for comparison across animals (Figs. 2*G* and 3 *C* and *D*). To compare the width of this distribution, we calculated the points at which the distribution reached 50% of the maximum for each animal (Figs. 2*H* and 3 *E* and *F*). To analyze the proboscis placement relative to the occluded eyes of animals in experiment 4, we summed the proboscis contacts for the upper and lower half of the flower (along the long pattern axis) separately and mirrored one half to present the proboscis contacts relative to the pattern as they appear in the field of view of the animal (Fig. 4*E*).

Body alignment with the pattern. We determined the longitudinal body axis of the hawkmoths using the head and thorax tracking points in all video frames. Using these, we calculated the mean heading direction of the moths as the circular mean of frame-by-frame body axis orientations for the approach, probing, and departure phase (Fig. 2 *A–D*). The approach and departure data were obtained from a window of 250 ms directly before and after the probing phase on the flower. To make the calculations of the heading vector between the probing phase, which could be of variable length, comparable to that of the fixed-length approach and departure phases, the heading vector of the probing phase was calculated as a running average of 250 ms bin width. For the subsequent statistical analysis, we sorted the directions of all vectors with a vector length of more than 0.2 into 6 evenly spaced sectors (bin centers of 0°, ±60°, ±90°, ±120°, and 180°), relative to the line pattern's orientation.

Head movement analysis. We computed the magnitude squared coherence for various combinations of head tracking point movements and proboscis movements, to assess potential causality between head and proboscis movements by their temporal coincidence (*SI Appendix*, Fig. S6 *E* and *G–I*).

Random proboscis model. We generated a prediction where hawkmoths would place their proboscis solely based on flight movements. To achieve this, we extracted the hawkmoths' proboscis positions relative to their body, with the head–thorax body axis aligned to the y-axis of the coordinate system and the head positioned at the origin (Fig. 2*E*). We then randomly assigned proboscis positions from this distribution to body positions in each frame of a dataset corresponding to one condition, separately for each animal. By assigning existing proboscis positions relative to the animals' body, we preserved the relationship of the x and y coordinates of proboscis positions from the real trials. We generated 10 different iterations of the prediction for each animal (Fig. 2*F*). These predictions assume that the proboscis movements are random search movements and bear no relation to the pattern or the animals' relative position to the pattern at each point in time so that the proboscis placement relative to the pattern becomes purely a function of body movement–though with the spread of proboscis positions due to the proboscis' movement preserved (Fig. 2*G*, gray line). We further generated a model that assigned the mean position of the proboscis of each animal to the body position in each frame (Fig. 2*G*, dark purple line).

The density distribution of the hawkmoths' proboscis positions relative to their head–thorax axis while probing line patterns (*SI Appendix*, Fig. S4*H*) was also extracted for the subset of frames during which the hawkmoths' body was aligned (within 45° of the pattern, *SI Appendix*, Fig. S4*I*) or perpendicular (within

45° of the normal axis to the pattern, *SI Appendix*, Fig. S4*J*). The proboscis density distribution was normalized for each animal before averaging.

Proboscis movement analysis relative to the hawkmoths' body position. We further analyzed the hawkmoths' proboscis movements, transferred to the body's frame of reference as in the random proboscis model, yet keeping their temporal connection intact (*SI Appendix*, Fig. S3*A*). These movements reveal the range of motion and temporal structure of the movement of the hawkmoths' proboscis, independent of movements of the body, which are overlaid in the original tracking coordinates of the proboscis (Fig. 1*G*). To ground-truth our approach of isolating proboscis movements from the animals' body movements, we also extracted the Euclidian distance between the proboscis tip and the animals' head (*SI Appendix*, Fig. S3*A*), providing a separate measure for the movement of the proboscis parallel to the animals' body axis. We calculated the amplitude spectrum of the parallel and perpendicular to the body axis component of the isolated proboscis movements (*SI Appendix*, Fig. S3*B*), as well as of the distance of proboscis and head, to reveal the temporal frequency components of proboscis movement. We also calculated the ratio between the amplitude spectrum of the head–proboscis and the head–thorax distance, to isolate the movement frequencies that were characteristic for the proboscis, compared to the body (Fig. 1*H*).

We used the same analysis of proboscis movements in the body's frame of reference to compare the amplitude of proboscis movement parallel and perpendicular to the body's long axis in experiment 3 (Fig. 3 *G* and *H*). It should be noted that our analysis did not distinguish between active lateral proboscis movements and those that were caused by holding the proboscis stationary and moving the body around it. While the analysis thus illustrates the functional range of proboscis placements relative to the body's position, the amplitude of active lateral proboscis movements might be smaller than suggested by our analysis.

Proboscis movement analysis relative to the pattern. To analyze the relationship between the direction of proboscis movement and the orientation of the patterns' long axis, we calculated the mean vector of the proboscis' movement tracks on the flower for every probing trial of each animal (Fig. 4 *C* and *F*), using the Circular Statistics Toolbox for Matlab (51). For the subsequent statistical analysis, we sorted the directions of all vectors with a vector length greater than 0.2 into 6 evenly spaced sectors (bin centers of 0°, ±60°, ±90°, ±120°, and 180°), relative to the line pattern's orientation (bin centers of 0° and 180°).

Statistical analysis. For one-way statistical comparisons of paired data, we employed Wilcoxon signed-rank tests, while we used a Mann–Whitney rank-sum test to compare independent data.

To statistically analyze the alignment of the head–thorax body axis direction, as well as the proboscis probing track direction on the flower with the pattern orientation, we used generalized linear mixed-effects model in R v4.1.2 (R Foundation for Statistical Computing) using the package "lme4" with the formula

$$sector\ choice \sim (1 \mid animalID).$$

These estimated the probability of the body's heading or the proboscis' movement direction in a pattern or nonpattern sector–scored for each individual trial as 0 or 1, accounting for individual animal biases. The random choice probability for the line pattern was 0.33.

The detailed results of all statistical comparisons are either directly presented with the figures, where this was possible, or presented in *SI Appendix*, Tables S1–S5, where the statistical comparisons were more extensive.

Data, Materials, and Software Availability. The raw tracking data of all hawkmoths in all experiments, as well as images of all eyes before and after obstruction with paint, are publicly available in a Figshare repository (DOI: 10.6084/m9.figshare.22639981.v1) (52). The detailed results of all statistical tests are presented in *SI Appendix*, Tables S1–S5. Custom-written computer code used to analyze the data is available in the GitHub repository https://github.com/annastoeckl/Code_Kannegieser_et_al_2024 (53).

ACKNOWLEDGMENTS. We acknowledge funding to A.S. from the Volkswagen Foundation (95490), the PostDoc Plus Program of the Graduate School of Life Sciences at the University of Würzburg, and the Bavarian Academy of Sciences and Humanities. We would like to thank Ilja Arent for his support in setting up the DeepLabCut environment in our group, Almut Kelber and Joaquín Goyret for their support and extremely helpful discussions at the start of this project, James Foster for support with the statistical analysis, and Franziska Schäfer and Christian Drerup for conducting experiments that inspired the conceptualization of experiments in this study.

1. A. P. Georgopoulos, S. Grillner, Visuomotor coordination in reaching and locomotion. *Science* **245**, 1209–1210 (1989).
2. A. Santamaria-Navarro, J. Solà, J. Andrade-Cetto, *Visual Guidance of Unmanned Aerial Manipulators* (Springer, 2019).
3. M. A. Goodale, Transforming vision into action. *Vision Res.* **51**, 1567–1587 (2011).
4. D. J. Kravitz, K. S. Saleem, C. I. Baker, M. Mishkin, A new neural framework for visuospatial processing. *Nat. Rev. Neurosci.* **12**, 217–230 (2011).
5. A. Pouget, L. H. Snyder, Computational approaches to sensorimotor transformations. *Nat. Neurosci.* **3**, 1192–1198 (2000).
6. C. Prablanc, M. Desmurget, H. Gréa, "Neural control of on-line guidance of hand reaching movements" in *Progress in Brain Research*, C. Prablanc, D. Pelisson, Y. Rossetti, Eds. (Neural Control of Space Coding and Action Production, Elsevier, 2003), vol. 142, pp. 155–170.
7. D. M. Clower *et al.*, Role of posterior parietal cortex in the recalibration of visually guided reaching. *Nature* **383**, 618–621 (1996).
8. D. Elliott *et al.*, The multiple process model of goal-directed reaching revisited. *Neurosci. Biobehav. Rev.* **72**, 95–110 (2017).
9. F. R. Sarlegna, P. K. Mutha, The influence of visual target information on the online control of movements. *Vision Res.* **110**, 144–154 (2015).
10. M. S. A. Graziano, G. S. Yap, C. G. Gross, Coding of visual space by premotor neurons. *Science* **266**, 1054–1057 (1994).
11. M. Kanai, H. Matsui, S. Watanabe, E. I. Izawa, Involvement of vision in tool use in crow. *NeuroReport* **25**, 1064–1068 (2014).
12. H. Matsui, E. I. Izawa, Flexible motor adjustment of pecking with an artificially extended bill in crows but not in pigeons. *R Soc. Open Sci.* **4**, 160796 (2017).
13. F. Bidel, N. C. Bennett, T. J. Wardill, Octopus bimaculoides' arm recruitment and use during visually evoked prey capture. *Curr. Biol.* **32**, 4727–4733.e3 (2022).
14. R. C. Feord *et al.*, Cuttlefish use stereopsis to strike at prey. *Sci. Adv.* **6**, eaay6036 (2020).
15. V. Nityananda *et al.*, A novel form of stereo vision in the praying mantis. *Curr. Biol.* **28**, 588–593.e4 (2018).
16. J. E. Niven, C. J. Buckingham, S. Lumley, M. F. Cuttle, S. B. Laughlin, Visual targeting of forelimbs in ladder-walking locusts. *Curr. Biol.* **20**, 86–91 (2010).
17. J. E. Niven, S. R. Ott, S. M. Rogers, Visually targeted reaching in horse-head grasshoppers. *Proc. R. Soc. B* **279**, 3697–3705 (2012).
18. S. Pick, R. Strauss, Goal-driven behavioral adaptations in gap-climbing Drosophila. *Curr. Biol.* **15**, 1473–1478 (2005).
19. S. Rossel, Spatial vision in the praying mantis: Is distance implicated in size detection? *J. Comp. Physiol. A* **169**, 101–108 (1991).
20. H. W. Honegger, A preliminary note on a new optomotor response in crickets: Antennal tracking of moving targets. *J. Comp. Physiol. A* **142**, 419–421 (1981).
21. S. Ye, V. Leung, A. Khan, Y. Baba, C. M. Comer, The antennal system and cockroach evasive behavior. I. Roles for visual and mechanosensory cues in the response. *J. Comp. Physiol. A* **189**, 89–96 (2003).
22. T. J. Prescott, M. E. Diamond, A. M. Wing, Active touch sensing. *Philos. Trans. R. Soc. B Biol. Sci.* **366**, 2989–2995 (2011).
23. T. Gutnick, R. A. Byrne, B. Hochner, M. Kuba, Octopus vulgaris uses visual information to determine the location of its arm. *Curr. Biol.* **21**, 460–462 (2011).
24. T. Matheson, Hindleg targeting during scratching in the locust. *J. Exp. Biol.* **200**, 93–100 (1997).
25. C. Schütz, V. Dürr, Active tactile exploration for adaptive locomotion in the stick insect. *Philos. Trans. R. Soc. B Biol. Sci.* **366**, 2996–3005 (2011).
26. J. Goyret, Look and touch: Multimodal sensory control of flower inspection movements in the nocturnal hawkmoth Manduca sexta. *J. Exp. Biol.* **213**, 3676–3682 (2010).
27. J. Goyret, A. Kelber, How does a diurnal hawkmoth find nectar? Differences in sensory control with a nocturnal relative. *Behav. Ecol.* **22**, 976–984 (2011).
28. J. Goyret, A. Kelber, Chromatic signals control proboscis movements during hovering flight in the hummingbird hawkmoth Macroglossum stellatarum. *PLoS One* **7**, e34629 (2012).
29. T. Deora, M. A. Ahmed, T. L. Daniel, B. W. Brunton, Tactile active sensing in an insect plant pollinator. *J. Exp. Biol.* **224**, jeb239442 (2021).
30. A. L. Stöckl, A. Kelber, Fuelling on the wing: Sensory ecology of hawkmoth foraging. *J. Comp. Physiol. A.* **205**, 399–413 (2019).
31. H. W. Krenn, Functional morphology and movements of the proboscis of Lepidoptera (Insecta). *Zoomorphology* **110**, 105–114 (1990).
32. H. W. Krenn, Feeding mechanisms of adult Lepidoptera: Structure, function, and evolution of the mouthparts. *Annu. Rev. Entomol.* **55**, 307–327 (2010).
33. G. Wannenmacher, L. T. Wasserthal, Contribution of the maxillary muscles to proboscis movement in hawkmoths (Lepidoptera: Sphingidae)–an electrophysiological study. *J. Insect Physiol.* **49**, 765–776 (2003).
34. S. Sponberg, J. P. Dyhr, R. W. Hall, T. L. Daniel, Luminance-dependent visual processing enables moth flight in low light. *Science* **348**, 1245–1248 (2015).
35. A. L. Stöckl, K. Kihlström, S. Chandler, S. Sponberg, Comparative system identification of flower tracking performance in three hawkmoth species reveals adaptations for dim light vision. *Phil. Trans. R. Soc. Lond. B.* **372**, 20160078 (2017).
36. A. R. Sobinov, S. J. Bensmaia, The neural mechanisms of manual dexterity. *Nat. Rev. Neurosci.* **22**, 741–757 (2021).
37. E. Roth, R. W. Hall, T. L. Daniel, S. Sponberg, Integration of parallel mechanosensory and visual pathways resolved through sensory conflict. *Proc. Natl. Acad. Sci. U.S.A.* **113**, 12832–12837 (2016).
38. J. Copeland, A. D. Carlson, Prey capture in mantids: A non-stereotyped component of lunge. *J. Insect Physiol.* **25**, 263–269 (1979).
39. B. J. Corrette, Prey capture in the praying mantis Tenodera aridifolia sinensis: Coordination of the capture sequence and strike movements. *J. Exp. Biol.* **148**, 147–180 (1990).

40. F.R. Prete, K.S. Cleal, The predatory strike of free ranging praying mantises, Sphodromantis lineola (Burmeister). I: Strikes in the mid-sagittal plane. *Brain. Behav. Evol.* **48**, 173–190 (1996).
41. J. D. Crawford, W. P. Medendorp, J. J. Marotta, Spatial transformations for eyehand coordination. *J. Neurophysiol.* **92**, 10–19 (2004).
42. E. J. Warrant, Seeing better at night: Life style, eye design and the optimum strategy of spatial and temporal summation. *Vision Res.* **39**, 1611–1630 (1999).
43. A. L. Stöckl, D. C. O'Carroll, E. Warrant, Higher-order neural processing tunes motion neurons to visual ecology in three species of hawkmoths. *Proc. R. Soc. B.* **284**, 20170880 (2017).
44. J. A. Saunders, D. C. Knill, Humans use continuous visual feedback from the hand to control fast reaching movements. *Exp. Brain Res.* **152**, 341–352 (2003).
45. J. A. Saunders, D. C. Knill, Visual feedback control of hand movements. *J. Neurosci.* **24**, 3223–3234 (2004).
46. R. W. Langridge, J. J. Marotta, Grasping occluded targets: Investigating the influence of target visibility, allocentric cue presence, and direction of motion on gaze and grasp accuracy. *Exp. Brain Res.* **235**, 2705–2716 (2017).
47. F. Ruggiero, V. Lippiello, A. Ollero, Aerial manipulation: A literature review. *IEEE Robot. Autom. Lett.* **3**, 1957–1964 (2018).
48. A. Kelber, Innate preferences for flower features in the hawkmoth Macroglossum stellatarum. *J. Exp. Biol.* **200**, 827–836 (1997).
49. A. Mathis *et al.*, DeepLabCut: Markerless pose estimation of user-defined body parts with deep learning. *Nat. Neurosci.* **21**, 1281 (2018).
50. T. L. Hedrick, Software techniques for two- and three-dimensional kinematic measurements of biological and biomimetic systems. *Bioinspir. Biomim.* **3**, 034001 (2008).
51. P. Berens, CircStat: A MATLAB toolbox for cdircular statistics. *J. Stat. Softw.* **31**, 1–21 (2009).
52. S. Kannegieser, N. Kraft, A. Haan, A. Stöckl, Visual guidance fine-tunes probing movements of an insect appendage. Figshare. Dataset. https://doi.org/10.6084/m9.figshare.22639981.v1. Deposited 18 December 2023.
53. S. Kannegieser, N. Kraft, A. Haan, A. Stöckl, Code_Kannegieser_et_al_2024. Github. Repository. https://github.com/annastoeckl/Code_Kannegieser_et_al_2024. Deposited 20 December 2023.